

Redetermination of AgPO_3

Katherine V. Terebilenko,^{a*} Igor V. Zatovsky,^a Ivan V. Ogorodnyk,^a Vyacheslav N. Baumer^b and Nikolay S. Slobodyanik^a

^aDepartment of Inorganic Chemistry, Taras Shevchenko National University, 64 Volodymyrska Street, 01601 Kyiv, Ukraine, and ^bSTC 'Institute for Single Crystals', NAS of Ukraine, 60 Lenin Avenue, 61001 Kharkiv, Ukraine

Correspondence e-mail: tereb@bigmir.ru

Received 19 January 2011; accepted 31 January 2011

Key indicators: single-crystal X-ray study; $T = 293\text{ K}$; mean $\sigma(\text{P}-\text{O}) = 0.002\text{ \AA}$; R factor = 0.024; wR factor = 0.058; data-to-parameter ratio = 25.4.

Single crystals of silver(I) polyphosphate(V), AgPO_3 , were prepared via a phosphoric acid melt method using a solution of Ag_3PO_4 in H_3PO_4 . In comparison with the previous study based on single-crystal Weissenberg photographs [Jost (1961). *Acta Cryst.* **14**, 779–784], the results were mainly confirmed, but with much higher precision and with all displacement parameters refined anisotropically. The structure is built up from two types of distorted edge- and corner-sharing $[\text{AgO}_5]$ polyhedra, giving rise to multidirectional ribbons, and from two types of PO_4 tetrahedra linked into meandering chains $(\text{PO}_3)_n$ spreading parallel to the b axis with a repeat unit of four tetrahedra. The calculated bond-valence sum value of one of the two Ag^+ ions indicates a significant strain of the structure.

Related literature

For a previous crystallographic study of AgPO_3 , see: Jost (1961). For the isotopic A-form of the Kurrol salt NaPO_3 , see: McAdam *et al.* (1968). Properties of glassy silver phosphates have been reported by Portier *et al.* (1990) and Novita *et al.* (2009). For long-chain polyphosphates $\text{AgM}^{\text{III}}(\text{PO}_3)_4$ ($M^{\text{III}} = \text{La, Gd, Eu}$), see: El Masloumi *et al.* (2005); Naili *et al.* (2006); Ayadi *et al.* (2009). For $\text{AgM}^{\text{II}}(\text{PO}_3)_3$ ($M^{\text{II}} = \text{Mg, Zn, Ba}$), see: Belharouak *et al.* (1999); for $\text{AgM}^{\text{I}}(\text{PO}_3)_2$ ($M^{\text{I}} = \text{K, Rb, Cs, Tl}$), see: Averbuch-Pouchot (1993). For background to the bond-valence method, see: Brown & Altermatt (1985).

Experimental

Crystal data

AgPO_3	$c = 7.3278(2)\text{ \AA}$
$M_r = 186.84$	$\beta = 93.491(2)^\circ$
Monoclinic, $P2_1/n$	$V = 529.53(2)\text{ \AA}^3$
$a = 11.9335(3)\text{ \AA}$	$Z = 8$
$b = 6.0667(1)\text{ \AA}$	Mo $K\alpha$ radiation

$\mu = 7.96\text{ mm}^{-1}$
 $T = 293\text{ K}$

$0.10 \times 0.08 \times 0.04\text{ mm}$

Data collection

Oxford Diffraction Xcalibur-3 CCD diffractometer
Absorption correction: multi-scan (Blessing, 1995)
 $T_{\min} = 0.465$, $T_{\max} = 0.733$

22720 measured reflections
2333 independent reflections
2208 reflections with $I > 2\sigma(I)$
 $R_{\text{int}} = 0.042$

Refinement

$R[F^2 > 2\sigma(F^2)] = 0.024$
 $wR(F^2) = 0.058$
 $S = 1.08$
2333 reflections

92 parameters
 $\Delta\rho_{\max} = 1.43\text{ e \AA}^{-3}$
 $\Delta\rho_{\min} = -1.86\text{ e \AA}^{-3}$

Table 1
Selected geometric parameters (\AA , $^\circ$).

$\text{Ag1}-\text{O3}^{\text{i}}$	2.441 (2)	$\text{Ag2}-\text{O3}^{\text{iv}}$	2.750 (2)
$\text{Ag1}-\text{O1}$	2.460 (2)	$\text{P1}-\text{O1}$	1.490 (2)
$\text{Ag1}-\text{O6}^{\text{ii}}$	2.491 (2)	$\text{P1}-\text{O3}$	1.4952 (19)
$\text{Ag1}-\text{O1}^{\text{iii}}$	2.511 (2)	$\text{P1}-\text{O4}^{\text{vi}}$	1.5889 (17)
$\text{Ag1}-\text{O6}$	2.540 (2)	$\text{P1}-\text{O2}$	1.6033 (17)
$\text{Ag2}-\text{O5}^{\text{iv}}$	2.3708 (19)	$\text{P2}-\text{O5}$	1.479 (2)
$\text{Ag2}-\text{O5}^{\text{v}}$	2.3756 (19)	$\text{P2}-\text{O6}$	1.4924 (19)
$\text{Ag2}-\text{O3}$	2.3968 (19)	$\text{P2}-\text{O4}$	1.5909 (17)
$\text{Ag2}-\text{O6}^{\text{ii}}$	2.487 (2)	$\text{P2}-\text{O2}$	1.6074 (18)
$\text{P1}-\text{O2}-\text{P2}$	124.88 (11)	$\text{P1}^{\text{vii}}-\text{O4}-\text{P2}$	135.91 (11)

Symmetry codes: (i) $x, y - 1, z$; (ii) $-x, -y + 1, -z + 1$; (iii) $-x + \frac{1}{2}, y - \frac{1}{2}, -z + \frac{3}{2}$; (iv) $-x, -y + 2, -z + 1$; (v) $x, y, z + 1$; (vi) $-x + \frac{1}{2}, y + \frac{1}{2}, -z + \frac{1}{2}$; (vii) $-x + \frac{1}{2}, y - \frac{1}{2}, -z + \frac{1}{2}$.

Data collection: *CrysAlis CCD* (Oxford Diffraction, 2006); cell refinement: *CrysAlis CCD*; data reduction: *CrysAlis RED* (Oxford Diffraction, 2006); program(s) used to solve structure: *SHELXS97* (Sheldrick, 2008); program(s) used to refine structure: *SHELXL97* (Sheldrick, 2008); molecular graphics: *DIAMOND* (Brandenburg, 1999); software used to prepare material for publication: *WinGX* (Farrugia, 1999) and *enCIFer* (Allen *et al.*, 2004).

Supplementary data and figures for this paper are available from the IUCr electronic archives (Reference: WM2454).

References

- Allen, F. H., Johnson, O., Shields, G. P., Smith, B. R. & Towler, M. (2004). *J. Appl. Cryst.* **37**, 335–338.
Averbuch-Pouchot, M. T. (1993). *J. Solid State Chem.* **102**, 93–99.
Ayadi, M., Férid, M. & Moine, B. (2009). *Acta Cryst. E65*, i13.
Belharouak, I., Aouad, H., Mesnaoui, M., Maazaz, M., Parent, C., Tanguy, B., Gravereau, P. & Le Flem, G. (1999). *J. Solid State Chem.* **145**, 97–103.
Blessing, R. H. (1995). *Acta Cryst. A51*, 33–38.
Brandenburg, K. (1999). *DIAMOND*. Crystal Impact GbR, Bonn, Germany.
Brown, I. D. & Altermatt, D. (1985). *Acta Cryst. B41*, 244–247.
El Masloumi, M., Imaz, I., Chaminade, J.-P., Videau, J.-J., Couzi, M., Mesnaoui, M. & Maazaz, M. (2005). *J. Solid State Chem.* **178**, 3581–3588.
Farrugia, L. J. (1999). *J. Appl. Cryst.* **32**, 837–838.
Jost, K. H. (1961). *Acta Cryst.* **14**, 779–784.
McAdam, A., Jost, K. H. & Beagley, B. (1968). *Acta Cryst. B24*, 1621–1622.
Naili, H., Ettis, H. & Mhiri, T. (2006). *J. Alloys Compd.* **424**, 400–407.
Novita, D. I., Boolchand, P., Malki, M. & Micoulaut, M. (2009). *J. Phys. Condens. Matter*, **21**, 205106.
Oxford Diffraction (2006). *CrysAlis CCD* and *CrysAlis RED*. Oxford Diffraction Ltd, Abingdon, England.
Portier, L. J., Tanguy, B., Videau, J. J., Allal, M. A. A., Morcos, J. & Salardenne, J. (1990). *Active Passive Elec. Compd.* **14**, 81–94.
Sheldrick, G. M. (2008). *Acta Cryst. A64*, 112–122.

supplementary materials

Acta Cryst. (2011). E67, i22 [doi:10.1107/S1600536811003977]

Redetermination of AgPO₃

K. V. Terebilenko, I. V. Zatovsky, I. V. Ogorodnyk, V. N. Baumer and N. S. Slobodyanik

Comment

Glassy silver polyphosphates as a part of complex oxide-chalcogenide systems have various applications in the field of solid electrolytes (Portier *et al.*, 1990; Novita *et al.*, 2009). Much attention has therefore been paid to phase equilibrium studies within AgPO₃-M(PO₃)_n systems, where M is a rare earth (Ayadi *et al.*, 2009; Naili *et al.*, 2006, El Masloumi *et al.*, 2005), a divalent (Belharouak *et al.*, 1999) or a monovalent metal (Averbuch-Pouchot, 1993).

The title compound is isotypic with the *A*-form of the Kurrol salt NaPO₃ (McAdam *et al.*, 1968). AgPO₃ has been previously structurally studied based on single crystal Weissenberg photographs (Jost, 1961). The current study mainly confirms the previous results, but with significantly higher precision and with anisotropic displacement parameters refined for all atoms.

The structure of AgPO₃ features two types of penta-coordinated Ag^I ions: Ag1 is located in a distorted trigonal bipyramidal and Ag2 in a irregular tetragonal pyramid of oxygen atoms (Fig. 1). Calculated values of bond valence sums (BVS; Brown & Altermatt, 1985) were found to be quite different: 0.96 valence units (v.u.) for Ag2 and 0.87 v.u. for Ag1. The observed deviation of the BVS of the latter atom from its chemical valence (expected 1) is due to a high polyhedral distortion caused by the presence of rigid (PO₃)_n chains. In this case the BVS values may be seen as a degree of silver "underbonding" and have a concomitant effect on physical properties of the title compound or glassy materials containing silver polyphosphate. The next-nearest coordination spheres of Ag1 include six adjacent silver atoms, resulting in edge-sharing Ag1 and Ag2 polyhedra and other four polyhedra connected through corners. As a result of this linkage, two polyhedral ribbons appear. One spreads parallel to the *a*-axis through interconnected [Ag1O₅] polyhedra by sharing a common edge and vertex alternatively, and another spreads parallel to the *b*-axis and consist of corner-sharing [Ag1O₅] polyhedra. Ag2 is remotely surrounded by one Ag1 and two Ag2, resulting in a ribbon of edge-sharing [Ag2O₅] polyhedra that run parallel to the *c*-axis. Intersecting these ribbons leads to a three-dimensional network penetrated with tunnels having eight-sided windows. Helical chains (PO₃)_n with a repeating unit of four phosphate tetrahedra are located within the tunnels and spiral along the 2₁ axes parallel to the *b*-axis. Due to the centrosymmetric nature of the structure, adjacent chains are left- and right-helices. As is characteristic for *catena*-polyphosphates (Averbuch-Pouchot, 1993), each of the two PO₄ tetrahedra displays two types of P—O bond lengths: P—O terminal ranging from 1.479 (2) to 1.4952 (19) Å and P—O bridging from 1.5889 (17) to 1.6074 (18) Å. The corresponding BVS are 4.92 v.u. and 4.95 v.u. for P1 and P2, respectively. The BVS per doubled formula (corresponds to the crystallographically independent atoms in a cell) of positively charged atoms equals to 11.72 v.u., while the chemical charge of the remaining O atoms is equal to -12 valences. This difference is an additional indication of the strain in the structure caused by the presence of rigid phosphate chains.

supplementary materials

Experimental

AgPO_3 was prepared by crystallizing a solution of Ag_3PO_4 in H_3PO_4 (84 %_{wt}) at a molar ratio $\text{Ag}/\text{P} = 0.01$. The thermal treatment included heating the mixture in a graphite crucible at 473 K for 6 h and then cooling to room temperature. After leaching with water, the product consisted of colorless prismatic crystals.

Refinement

The highest peak and the deepest hole in the final difference map are located at 0.56 Å from Ag1 ($1.432 \text{ e}/\text{\AA}^3$) and 0.56 Å from Ag1 ($-1.858 \text{ e}/\text{\AA}^3$), respectively

Figures

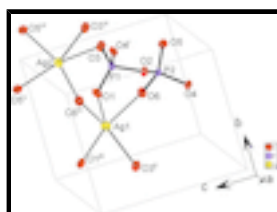


Fig. 1. The connectivity of the Ag and P atoms in the structure of AgPO_3 with displacement ellipsoids displayed at the 50% probability level. [Symmetry codes: (i) $0.5 - x, 1/2 + y, 0.5 - z$; (ii) $-x, -1 + y, z$; (iii) $0.5 - x, 1/2 + y, 1.5 - z$; (iv) $-x, 1 - y, 1 - z$; (v) $x, y, 1 + z$; (vi) $-x, 2 - y, 1 - z$].

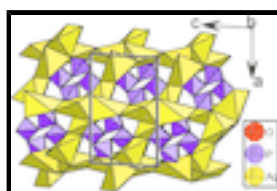


Fig. 2. A view of the crystal structure of AgPO_3 down the b -axis, emphasizing the tunnels with eight-sided windows where the helical polyphosphate chains reside.

Silver(I) polyphosphate

Crystal data

AgPO_3	$F(000) = 688$
$M_r = 186.84$	$D_x = 4.687 \text{ Mg m}^{-3}$
Monoclinic, $P2_1/n$	Mo $K\alpha$ radiation, $\lambda = 0.71073 \text{ \AA}$
Hall symbol: -P 2yn	Cell parameters from 22720 reflections
$a = 11.9335 (3) \text{ \AA}$	$\theta = 3.2\text{--}35.0^\circ$
$b = 6.0667 (1) \text{ \AA}$	$\mu = 7.96 \text{ mm}^{-1}$
$c = 7.3278 (2) \text{ \AA}$	$T = 293 \text{ K}$
$\beta = 93.491 (2)^\circ$	Prism, colorless
$V = 529.53 (2) \text{ \AA}^3$	$0.10 \times 0.08 \times 0.04 \text{ mm}$
$Z = 8$	

Data collection

Oxford Diffraction Xcalibur-3 CCD diffractometer	2333 independent reflections
Radiation source: fine-focus sealed tube	2208 reflections with $I > 2\sigma(I)$

graphite	$R_{\text{int}} = 0.042$
φ and ω scans	$\theta_{\text{max}} = 35^\circ, \theta_{\text{min}} = 3.2^\circ$
Absorption correction: multi-scan (Blessing, 1995)	$h = -19 \rightarrow 19$
$T_{\text{min}} = 0.465, T_{\text{max}} = 0.733$	$k = -9 \rightarrow 9$
22720 measured reflections	$l = -11 \rightarrow 11$

Refinement

Refinement on F^2	Primary atom site location: structure-invariant direct methods
Least-squares matrix: full	Secondary atom site location: difference Fourier map
$R[F^2 > 2\sigma(F^2)] = 0.024$	$w = 1/[\sigma^2(F_o^2) + (0.0212P)^2 + 1.7313P]$ where $P = (F_o^2 + 2F_c^2)/3$
$wR(F^2) = 0.058$	$(\Delta/\sigma)_{\text{max}} = 0.001$
$S = 1.08$	$\Delta\rho_{\text{max}} = 1.43 \text{ e \AA}^{-3}$
2333 reflections	$\Delta\rho_{\text{min}} = -1.86 \text{ e \AA}^{-3}$
92 parameters	Extinction correction: <i>SHELXL97</i> (Sheldrick, 2008)
0 restraints	Extinction coefficient: 0.0034 (3)

Special details

Geometry. All e.s.d.'s (except the e.s.d. in the dihedral angle between two l.s. planes) are estimated using the full covariance matrix. The cell e.s.d.'s are taken into account individually in the estimation of e.s.d.'s in distances, angles and torsion angles; correlations between e.s.d.'s in cell parameters are only used when they are defined by crystal symmetry. An approximate (isotropic) treatment of cell e.s.d.'s is used for estimating e.s.d.'s involving l.s. planes.

Refinement. Refinement of F^2 against ALL reflections. The weighted R -factor wR and goodness of fit S are based on F^2 , conventional R -factors R are based on F , with F set to zero for negative F^2 . The threshold expression of $F^2 > \sigma(F^2)$ is used only for calculating R -factors(gt) etc. and is not relevant to the choice of reflections for refinement. R -factors based on F^2 are statistically about twice as large as those based on F , and R -factors based on ALL data will be even larger.

Fractional atomic coordinates and isotropic or equivalent isotropic displacement parameters (\AA^2)

	x	y	z	$U_{\text{iso}}^*/U_{\text{eq}}$
Ag1	0.127313 (18)	0.33468 (3)	0.61230 (3)	0.02461 (6)
Ag2	0.03023 (2)	0.89757 (4)	0.77035 (3)	0.02748 (6)
P1	0.22766 (5)	0.81768 (10)	0.48624 (7)	0.01372 (10)
P2	0.11152 (5)	0.61417 (10)	0.18002 (8)	0.01331 (10)
O1	0.25346 (18)	0.6554 (3)	0.6355 (3)	0.0241 (4)
O2	0.22388 (14)	0.6980 (3)	0.2909 (2)	0.0179 (3)
O3	0.12509 (15)	0.9578 (3)	0.4956 (3)	0.0218 (3)
O4	0.16402 (14)	0.4679 (3)	0.0265 (2)	0.0169 (3)
O5	0.05294 (17)	0.7997 (3)	0.0843 (3)	0.0234 (3)
O6	0.04724 (16)	0.4744 (3)	0.3047 (3)	0.0220 (3)

supplementary materials

Atomic displacement parameters (\AA^2)

	U^{11}	U^{22}	U^{33}	U^{12}	U^{13}	U^{23}
Ag1	0.02707 (10)	0.02043 (10)	0.02611 (10)	0.00056 (7)	-0.00023 (7)	0.00252 (7)
Ag2	0.03883 (12)	0.02340 (11)	0.02121 (9)	0.00423 (8)	0.01011 (8)	0.00068 (7)
P1	0.0138 (2)	0.0153 (2)	0.0121 (2)	-0.00206 (17)	0.00169 (16)	0.00000 (17)
P2	0.0124 (2)	0.0141 (2)	0.0134 (2)	0.00133 (17)	0.00096 (16)	-0.00069 (17)
O1	0.0312 (9)	0.0223 (9)	0.0183 (7)	-0.0081 (7)	-0.0021 (7)	0.0064 (6)
O2	0.0155 (6)	0.0225 (8)	0.0157 (6)	-0.0010 (6)	0.0008 (5)	-0.0059 (6)
O3	0.0169 (7)	0.0268 (9)	0.0220 (8)	0.0031 (6)	0.0041 (6)	-0.0047 (7)
O4	0.0161 (6)	0.0200 (8)	0.0145 (6)	0.0058 (6)	0.0000 (5)	-0.0042 (5)
O5	0.0278 (9)	0.0208 (8)	0.0211 (8)	0.0108 (7)	-0.0020 (6)	0.0000 (6)
O6	0.0218 (8)	0.0243 (9)	0.0204 (7)	-0.0050 (7)	0.0061 (6)	0.0000 (7)

Geometric parameters (\AA , $^\circ$)

Ag1—O3 ⁱ	2.441 (2)	P1—O4 ^{vii}	1.5889 (17)
Ag1—O1	2.460 (2)	P1—O2	1.6033 (17)
Ag1—O6 ⁱⁱ	2.491 (2)	P2—O5	1.479 (2)
Ag1—O1 ⁱⁱⁱ	2.511 (2)	P2—O6	1.4924 (19)
Ag1—O6	2.540 (2)	P2—O4	1.5909 (17)
Ag1—Ag2 ⁱ	3.1431 (3)	P2—O2	1.6074 (18)
Ag2—O5 ^{iv}	2.3708 (19)	O1—Ag1 ^{viii}	2.511 (2)
Ag2—O5 ^v	2.3756 (19)	O3—Ag1 ^{vi}	2.441 (2)
Ag2—O3	2.3968 (19)	O4—P1 ^{ix}	1.5889 (17)
Ag2—O6 ⁱⁱ	2.487 (2)	O5—Ag2 ^{iv}	2.3708 (19)
Ag2—O3 ^{iv}	2.750 (2)	O5—Ag2 ^x	2.3756 (19)
Ag2—Ag1 ^{vi}	3.1431 (3)	O6—Ag2 ⁱⁱ	2.487 (2)
P1—O1	1.490 (2)	O6—Ag1 ⁱⁱ	2.491 (2)
P1—O3	1.4952 (19)		
O3 ⁱ —Ag1—O1	139.36 (7)	O3—P1—O4 ^{vii}	110.36 (11)
O3 ⁱ —Ag1—O6 ⁱⁱ	121.99 (6)	O1—P1—O2	110.46 (11)
O1—Ag1—O6 ⁱⁱ	97.63 (7)	O3—P1—O2	108.66 (10)
O3 ⁱ —Ag1—O1 ⁱⁱⁱ	81.11 (6)	O4 ^{vii} —P1—O2	100.72 (9)
O1—Ag1—O1 ⁱⁱⁱ	88.56 (4)	O5—P2—O6	118.48 (12)
O6 ⁱⁱ —Ag1—O1 ⁱⁱⁱ	117.80 (6)	O5—P2—O4	106.52 (10)
O3 ⁱ —Ag1—O6	90.36 (7)	O6—P2—O4	110.79 (11)
O1—Ag1—O6	89.59 (6)	O5—P2—O2	110.76 (12)
O6 ⁱⁱ —Ag1—O6	77.68 (6)	O6—P2—O2	108.33 (10)
O1 ⁱⁱⁱ —Ag1—O6	164.51 (6)	O4—P2—O2	100.46 (9)
O3 ⁱ —Ag1—Ag2 ⁱ	48.87 (5)	P1—O1—Ag1	111.96 (11)
O1—Ag1—Ag2 ⁱ	151.61 (4)	P1—O1—Ag1 ^{viii}	109.67 (10)
O6 ⁱⁱ —Ag1—Ag2 ⁱ	88.27 (5)	Ag1—O1—Ag1 ^{viii}	135.28 (8)

O1 ⁱⁱⁱ —Ag1—Ag2 ⁱ	64.42 (5)	P1—O2—P2	124.88 (11)
O6—Ag1—Ag2 ⁱ	118.78 (4)	P1—O3—Ag2	112.45 (11)
O5 ^{iv} —Ag2—O5 ^v	77.57 (7)	P1—O3—Ag1 ^{vi}	123.86 (11)
O5 ^{iv} —Ag2—O3	119.43 (7)	Ag2—O3—Ag1 ^{vi}	81.04 (6)
O5 ^v —Ag2—O3	145.04 (7)	P1 ^{ix} —O4—P2	135.91 (11)
O5 ^{iv} —Ag2—O6 ⁱⁱ	129.94 (7)	P2—O5—Ag2 ^{iv}	125.12 (11)
O5 ^v —Ag2—O6 ⁱⁱ	90.36 (7)	P2—O5—Ag2 ^x	132.23 (11)
O3—Ag2—O6 ⁱⁱ	98.10 (6)	Ag2 ^{iv} —O5—Ag2 ^x	102.43 (7)
O5 ^{iv} —Ag2—Ag1 ^{vi}	71.68 (5)	P2—O6—Ag2 ⁱⁱ	125.33 (11)
O5 ^v —Ag2—Ag1 ^{vi}	123.01 (5)	P2—O6—Ag1 ⁱⁱ	110.73 (11)
O3—Ag2—Ag1 ^{vi}	50.09 (5)	Ag2 ⁱⁱ —O6—Ag1 ⁱⁱ	99.83 (6)
O6 ⁱⁱ —Ag2—Ag1 ^{vi}	145.52 (4)	P2—O6—Ag1	123.59 (11)
O1—P1—O3	118.36 (12)	Ag2 ⁱⁱ —O6—Ag1	90.46 (7)
O1—P1—O4 ^{vii}	106.84 (10)	Ag1 ⁱⁱ —O6—Ag1	102.32 (6)

Symmetry codes: (i) $x, y-1, z$; (ii) $-x, -y+1, -z+1$; (iii) $-x+1/2, y-1/2, -z+3/2$; (iv) $-x, -y+2, -z+1$; (v) $x, y, z+1$; (vi) $x, y+1, z$; (vii) $-x+1/2, y+1/2, -z+1/2$; (viii) $-x+1/2, y+1/2, -z+3/2$; (ix) $-x+1/2, y-1/2, -z+1/2$; (x) $x, y, z-1$.

supplementary materials

Fig. 1

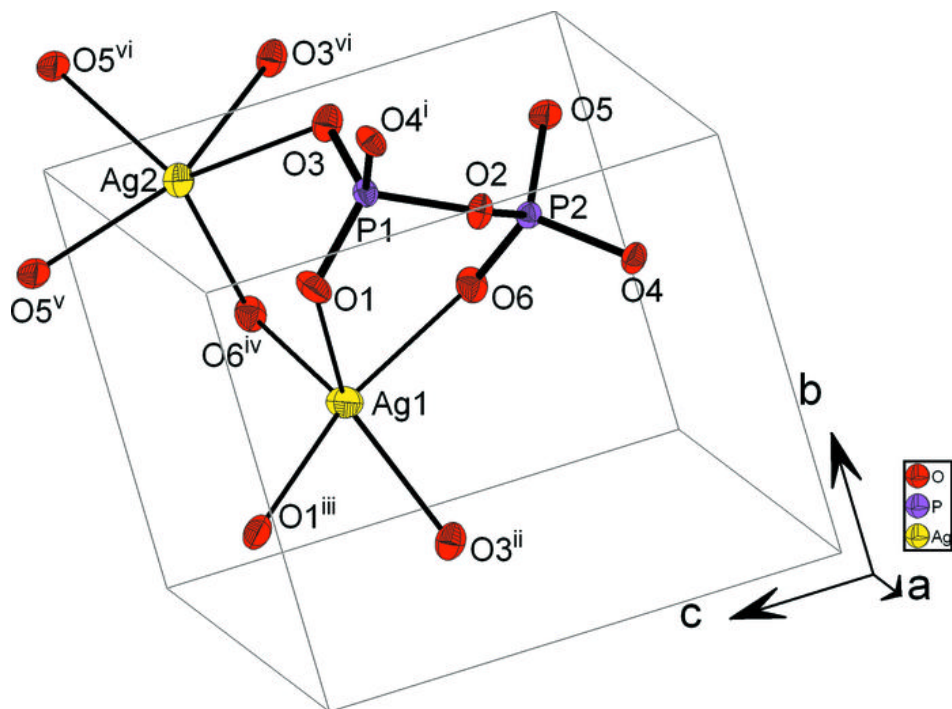


Fig. 2

